



Fluorine-free binders for carbon black based electrochemical supercapacitors

F. BECK and M. DOLATA

Universität Duisburg, Fachgebiet Elektrochemie, Lotharstr. 1, D-47057 Duisburg, Germany

Received 8 February 2000; accepted in revised form 12 December 2000

Key words: binder, carbon black, electrochemical supercapacitors, polymer dispersions, polystyrene/butadiene copolymers

Abstract

Industrially manufactured carbon blacks (CBs) provide highly dispersed carbon materials with a specific surface of up to $1700 \text{ m}^2 \text{ g}^{-1}$. Precompaction at $p > 10 \text{ MPa}$ in the presence of 3–10 wt % PTFE (provided as a dispersion) is known to lead to stable electrodes for electrochemical supercapacitors. Specific capacitances for single electrodes ($C_{s,1}$) were measured by constant current cycling (CCC) at 34 mA cm^{-2} to be up to 250 F g^{-1} . It is shown that substitution of PTFE by fluorine-free binders, such as aqueous dispersions of polystyrene, styrene/butadiene-copolymer and ethylene/acrylic acid copolymer is possible. Optimum systems were with 3–10 wt % binders of butadiene/styrene copolymers. They allowed stable results within hundreds of cycles. No shedding of the CB particles was observed, and swelling of the electrode was minimum.

1. Introduction

Electrochemical supercapacitors (ESCs) have specific capacitances, C_s , which exceed those of conventional capacitors by at least six orders of magnitude. This is due to the atomic dimensions of the electrochemical double layer. The specific capacitance for a single electrode, $C_{s,1}$, can be simply obtained from the double layer capacitance $C_{A,DL}$ after the atomic Helmholtz model and the specific surface A_s :

$$C_{s,1} = C_{A,DL} A_s \quad (1)$$

$C_{A,DL} = 10$ to $16 \mu\text{F cm}^{-2}$ holds for carbon [1, 2]. The C basal plane affords only $2 \mu\text{F cm}^{-2}$, and high values similar to metals (20 – $25 \mu\text{F cm}^{-2}$) are reported occasionally. Highly dispersed carbon is a very interesting material for the verification of electrochemical supercapacitors. Corrosion stability is excellent in acid electrolytes. Activated carbons (ACs) [3–5], and carbon blacks (CBs) [2, 6], were investigated in detail. The latter are produced industrially on a large scale according to the furnace process [7].

BET measurements lead to specific surfaces A_s for CBs of up to $1700 \text{ m}^2 \text{ g}^{-1}$. Particulate materials such as CB with a particle diameter of $d = 10 \text{ nm}$ would give a value of $A_s = 300 \text{ m}^2 \text{ g}^{-1}$ (density, $\rho \approx 2 \text{ g cm}^{-3}$) for compact nanoglobules according to the following equation:

$$A_s = \frac{6}{d\rho} \quad (2)$$

It is concluded that nanopores in the particles are responsible for the excess A_s [4, 8]. Figure 1 shows schematically the principal limitation of an electrochemical supercapacitor due to the onset of faradaic processes (i_F) at higher U/Q values.

A transformation to solid compact electrodes is necessary for practical applications. Monoblock electrodes are possible in special cases using carbon aerogels [9]. Sometimes a binder is omitted, and the pellet is held under permanent pressure [4]. But a binder is generally needed to accomplish a precompacted electrode from these powdery materials. Dispersions of PTFE [2, 3, 5, 6] are commonly used. An admixture of inexpensive methylcellulose has been reported [5]. The present paper describes the total elimination of PTFE by the introduction of novel fluorine free binders. These are interesting from the viewpoint of costs and environmental compatibility.

2. Experimental details

Table 1 shows some data for the five novel binders, which were acquired as aqueous dispersions. They did not contain fluorine. According to the chemical composition, no. 1 was an ethylene/acrylic acid-copolymer dispersion, no. 2 and no. 3 were polystyrene dispersions and no. 4 and no. 5 were butadiene/styrene copolymer dispersions. The reference PTFE-dispersion (DuPont, 59.9 wt % in water) was provided by C.H. Erbslöh, Krefeld/Germany.

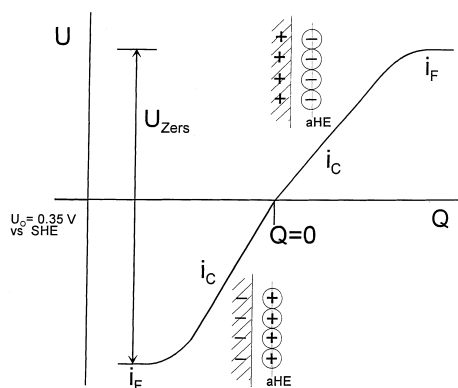


Fig. 1. Potential (U) against charge (Q) curves for the charge-discharge of a supercapacitor. Key: (i_c) capacitive currents, (i_F) faradaic currents, (U) potential, U_{Zers} decomposition voltage, (+) cation and (-) anion.

Three industrial CBs were employed, predominantly Ensaco E 62 MM ($A_s = 1500 \text{ m}^2 \text{ g}^{-1}$, $C_{s,1} = 200 \text{ F g}^{-1}$), in some cases Ensaco E 52 MM ($A_s = 1100 \text{ m}^2 \text{ g}^{-1}$, $C_{s,1} = 175 \text{ F g}^{-1}$) and Ensaco E 114 MM ($A_s = 1690 \text{ m}^2 \text{ g}^{-1}$, $C_{s,1} = 240 \text{ F g}^{-1}$). The carbon blacks were provided by Erachem Europe, Brussels (formerly MMM Carbon). The aqueous dispersions of the binders were diluted 1:10. In the next step, the CBs were thoroughly admixed by stirring. Thereafter, the water was evaporated at $110^\circ\text{C}/12 \text{ h}$ and finally at $80^\circ\text{C}/20 \text{ mbar}/20 \text{ h}$. A precompacted highly porous CB electrode was fabricated from the dry mixture at 440 MPa and 20°C . The diameter of the pellet was 1.7 cm ($A = 2.27 \text{ cm}^2$) and the thickness about 0.1 cm . The pellet made from E 52 MM exhibited a high density of 1.3 to 1.5 g cm^{-3} in the precompacted state, while the average density was 0.4 to 1.0 g cm^{-3} .

The pellet electrode was contacted by a Pt grid (from both sides) in an electrode holder with a titanium frame, cf. Figure 2. The Pt grid had 256 mesh cm^{-2} . In previous measurements pellets were enveloped in the Pt grid alone, cf. Figure 1 in [6].

Evaluation of the electrodes was performed by constant current cycling (CCC) in $12 \text{ M H}_2\text{SO}_4$ at 20°C , $j = 34 \text{ mA cm}^{-2}$ 100 cycles were standard. The reference

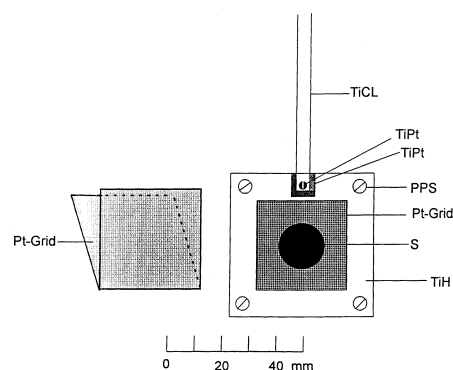


Fig. 2. Electrode (pellet) holder. Key: (S) sample (pellet), (TiCL) Ti-current lead, (TiH) Ti-frame, (PPS) polypropylene-screws and (TiPt) TiPt-screw or surface finish.

electrode was a $\text{Hg}/\text{Hg}_2\text{SO}_4$ electrode in $1 \text{ M H}_2\text{SO}_4$ (674 mV vs SHE). Potentials against this reference were denoted as U_s . Figure 3 shows an example of the CCC curves. The potential limits were $U_s = -0.3 \text{ V}$ and $+0.7 \text{ V}$, respectively, corresponding to the positive electrode of an ESC.

3. Results and discussion

As already noted, Figure 3 displays a sample CCC curve, $j = 34 \text{ mA cm}^{-2}$. It is rather close to the charge-discharge behaviour of a plate capacitor. Some steady state cycles around the 30th and 100th cycle are shown. The specific capacitance C_A is easily derived from the slope $v_s = dU/dt$ of the linear part:

$$C_A = \frac{j}{v_s} \quad (3)$$

The mass specific capacitance for a single electrode, $C_{s,1}$, is obtained therefrom by division by the mass of the

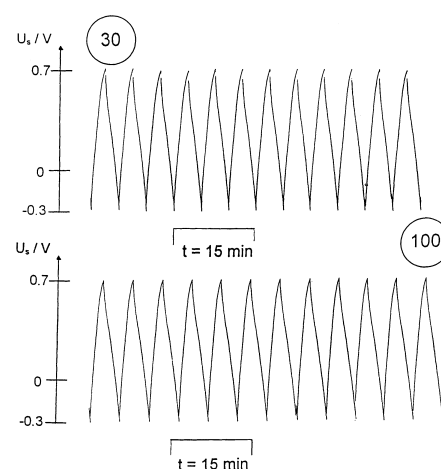


Fig. 3. Potential against time curves for CCC ($j = 34 \text{ mA cm}^{-2}$, $12 \text{ M H}_2\text{SO}_4$) of a carbon black (CB)/binder (B) composite electrode. CB = E 62 MM. B = Butonal LS 133 (no. 4 in Table 1). Pellet concentration c_B 10 wt %.

Table 1. Polymer dispersions: composition, solid concentration c_s in the dispersion and glass temperature T_g of the binder materials

Number*	Composition	Product mark (BASF)	c_s /wt %	T_g / $^\circ\text{C}$
1	Ethylene/acrylicacid copolymer dispersion	Poligen WE 3	25	
2	Polystyrene dispersion	Precursor T 6772	35	105
3	Polystyrene dispersion	Poligen ES 9676 X	50	105
4	Butadiene/styrene-copolymer dispersion	Butonal LS 133	64	-50
5	Styrene/butadiene copolymer dispersion	Styronal FX 8740 X	50	26

* Number used throughout

electrode. The supercapacitor contains two electrodes switched in series. $C_{s,c}$ of such a cell is obtained by division of $C_{s,1}$ by 4.

Figure 4 is the result of a further evaluation. It demonstrates that $C_{s,1}$ is reasonably constant within the first 100 cycles for binder 4 (Table 1). However, some loss is observed with respect to the run with the conventional PTFE binder. This loss is even stronger for lower binder concentrations, cf. Figure 5.

Figure 6(a) and (b) summarizes these results. This shows that the corresponding losses are obtained for all five novel binders. But a relative optimum is obtained for binders 2 and 4. On the other hand, the systems with the binders 3 and 4 are the only ones which exhibit total stability over the first 100 cycles.

An alternative carbon black, E 114 MM, with an extraordinarily high A_s of $1690 \text{ m}^2 \text{ g}^{-1}$ was chosen in long term runs for the optimum binder (no. 4) at two concentration levels. $C_{s,1}$ is accordingly larger. The results are presented in Figure 7.

The system can be safely cycled. The curve for the higher binder concentration is close to the PTFE curve. But the other lies considerably below it. An initial decay can be observed, which may be attributed to the alternative carbon black.

Finally, a third carbon black, E 52 MM, was applied in combination with some of the novel binders. This

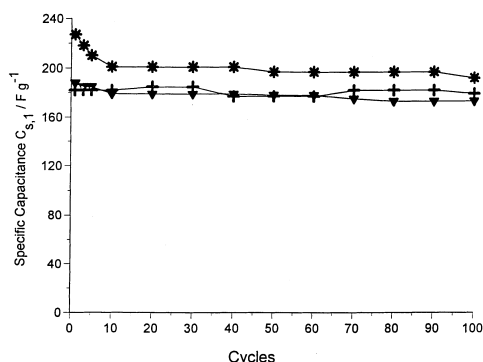


Fig. 4. Specific capacitances of single electrodes from Figure 3 in the course of first 100 cycles. Key: (∇ , $+$) two parallel runs, $m_{CB}=152$ and 139 mg , respectively, $c_B=10 \text{ wt } \%$; (*) $10 \text{ wt } \%$ PTFE as a binder.

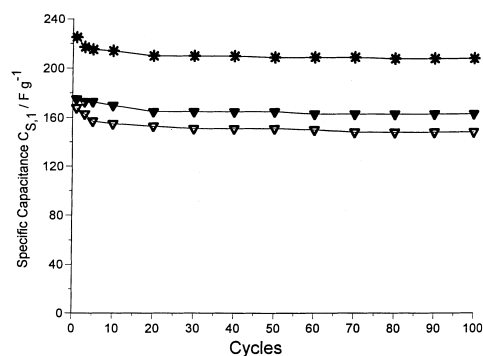


Fig. 5. Same as Figures 3 and 4, but (∇) $c_B=5 \text{ wt } \%$, (∇) $c_B=3 \text{ wt } \%$.

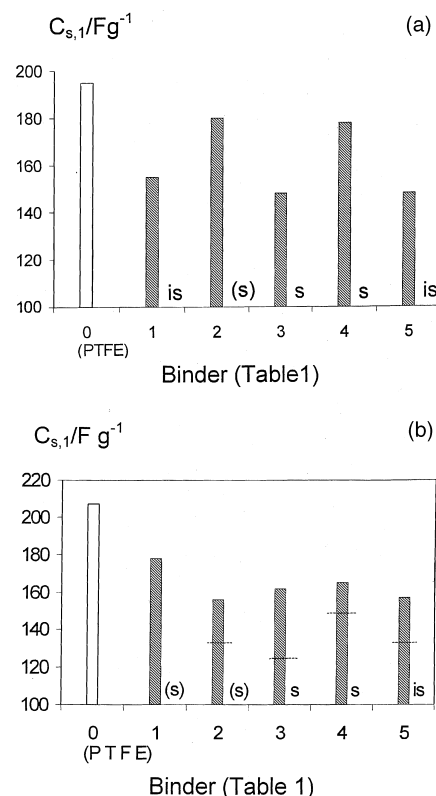


Fig. 6. $C_{s,1}$ data for PTFE (\square) and the five novel binders nos. 1–5 according to Table 1 (\blacksquare). (a) $c=10 \text{ wt } \%$; (b) $c=5 \text{ wt } \%$ (—) and $3 \text{ wt } \%$ (---). Carbon black: E 62 MM. Key: 's' = stable; '(s)' slightly unstable and 'is' = unstable on cycling.

carbon black is the only one among 25 samples [10] which led to a relatively high density of up to 1.5 g cm^{-3} as a precompacted pellet. In all the other cases, this density was much lower, namely in the range $0.4\text{--}1.0 \text{ g cm}^{-3}$.

Figure 8 shows a relative instability of these systems. Within the first 100 cycles, a pronounced decrease of $C_{s,1}$ was observed.

It is interesting to note that the diameter of the primary CB particles and the polymer particles of the binder dispersions differ by about one to two orders of magnitude. The structure of the porous pellet electrodes should therefore resemble, to some degree, that of the press/sinter materials [11]. A large particle of the

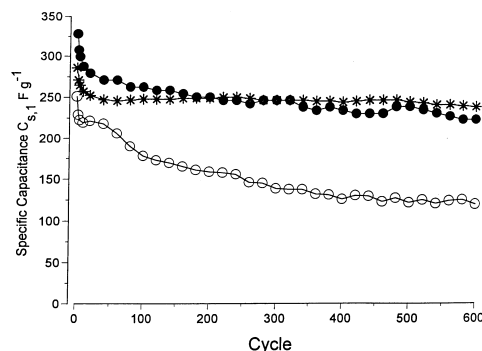


Fig. 7. Long term cycling of Carbon Black E 114 MM, Binder: Key: (*) PTFE, $c=10 \text{ wt } \%$; (\bullet) Butonal LS 133, no. 4, $c=10 \text{ wt } \%$; (\circ) Butonal LS 133, no. 4, $c=3 \text{ wt } \%$. Cycling conditions as in Figure 3.

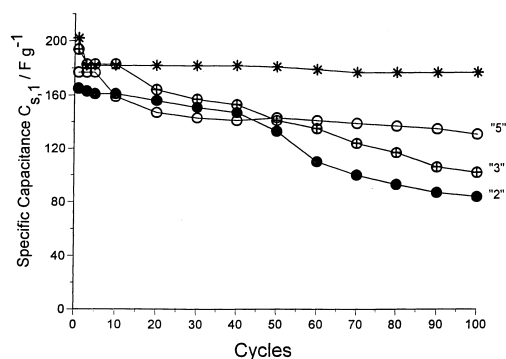


Fig. 8. Cycling of carbon black E 52, Binder ($c = 10$ wt %). Key: (*) PTFE; (●) no. 2, Table 1; (⊕) no. 3, Table 1; (○) no. 5, Table 1. Cycling conditions as in Figure 3.

polymer binder is coated with thick CB layers. Figure 9 is a schematic representation of that model. It is drawn with parameters which hold for dispersion no. 4 (Table 1), cf. legends.

The porosity of the carbon material is retained. But the cohesion of such a composite is difficult to understand. The loss of specific capacitance with respect to the PTFE binder may be attributed to the presence of low molecular weight components in the novel dispersions. These may be transported into the pores and lead to pore blocking. The cycling stability of system 4 is optimum. It is close to the conventional system with PTFE binder.

We could demonstrate, on the other hand, the possibility of such press/sinter materials for a high carbon black utilization. The first carbon black, Ensaco E 62 MM, was employed. A coarse polypropylene (Novolen) powder material (BASF) was used as a binder. It was milled in an achate ball mill at 0 °C for 5 min three times. The fraction 90–180 μm (30 wt %) was mixed with the carbon black (70 wt %), both as dry powders, and pressed at 100 MPa at two temperatures,

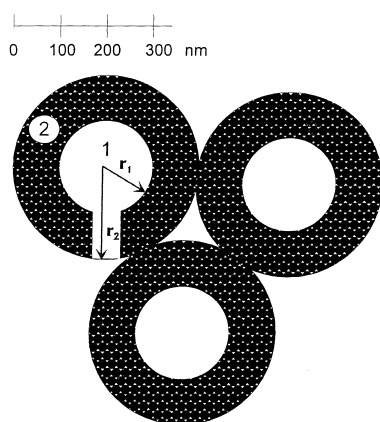


Fig. 9. Schematic representation of the carbon black electrode as a press/sinter-structure. 1, 2 are phases: (1) binder (polymer), (2) carbon black. ■ primary particles of the carbon black. The dimensions hold for the system no. 4, cf. Table 1. Average particle diameter of the dispersion of the binder is 200 nm. Diameter of the primary particles of the carbon black is 20 nm. Radius r_2 was calculated with the following data: 10 wt % binder, densities $\rho_1 = \rho_2 = 1$ g cm^{-3} .

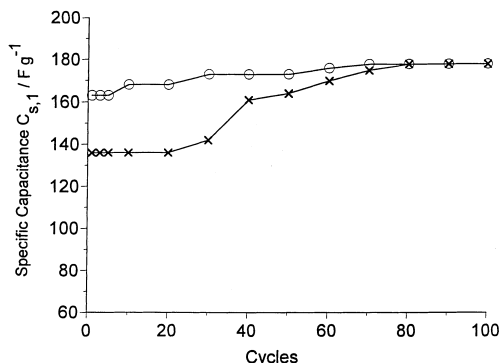


Fig. 10. Conducting press/sinter materials (see text). 30 wt % Novolen (PP); 70 wt % CB E 62 MM. Cycling conditions as in Figure 3. Key: (○) press-temperature (80 °C) and (x) press-temperature (120 °C).

80 and 120 °C. The composites had a reasonable mechanical strength.

Figure 10 shows the result of a CCC evaluation in 12 M H_2SO_4 under the same conditions as before. After 50–80 cycles of formation, a steady state was obtained. The formation period was longer for the sample, which was precompacted at the higher temperature. The final value of $C_{s,1}$, however, was close to that obtained with the best aqueous binder dispersions.

In conclusion, our results provide some insight into the role of the binder for the particular carbons which are employed for the electrode fabrication for ESCs. Even in the most comprehensive modern monograph on ESCs [12], this topic is not treated.

Acknowledgements

We are obliged to BASF Aktiengesellschaft, Ludwigshafen, (Dr Urban, Dr Röckel) for the provision of the binder dispersions (cf. Table 1), and to C.H. Erbslöh, Krefeld, for the PTFE dispersion. Our partner in the BRITE-Euram-Project, Erachem, Brussels (Dr Probst, Dr Grivei) provided the carbon blacks. We are grateful for this as well as for the financial support by the European Union (Project BE 96-3221).

References

1. K. Kinoshita, 'Carbon: Electrochemical and Physicochemical Properties' (J. Wiley & Sons, New York, 1988).
2. F. Krüger, PhD thesis, Universität Duisburg (1997), 'Entwicklung eines All-Kohlenstoff-Akkumulators in wässriger Schwefelsäure mit negativen Elektroden aus vorkompaktierten Industrierußen'.
3. M.F. Rose, C. Johnson, T. Owens and B. Stephens, *J. Power Sources* **47** (1994) 303.
4. H. Shi, *Electrochim. Acta* **41** (1996) 1633.
5. L. Bonnefoi, P. Simon, J.F. Fauvarque, C. Sarrazin, J.F. Sarrau and A. Dugast, *J. Power Sources* **80** (1999) 149.
6. F. Krüger and F. Beck, in V. Barsukov and F. Beck (Eds), 'New Promising Electrochemical Systems for Rechargeable Batteries' (Kluwer Academic, Dordrecht, 1996), pp. 373–389.
7. J.P. Donnet, R.C. Bansal and M. J. Wang (Eds), 'Carbon Black', 2nd edn (Marcel Dekker, New York, 1993).

8. K.S.W. Sing, 'Adsorption, Surface Area and Porosity', 2nd edn (Academic Publishers, London, 1982).
9. S.T. Mayer, R.W. Pekala and J.L. Kaschmitter, *J. Electrochem. Soc.* **140** (1993) 446.
10. F.Beck, F. Krüger and H. Krohn, *GDCh – Monographie* **12** (1998) 331.
11. R.G. Gilg, in H.J. Mair and S. Roth (Eds), 'Elektrisch leitende Kunststoffe' (Carl Hanser Verlag, München, 1989).
12. B.E. Conway, 'Electrochemical Supercapacitors; Scientific Fundamentals and Technological Applications' (Kluwer-Plenum, New York, 1999).